Composite Structures 265 (2021) 113501

Contents lists available at ScienceDirect

Composite Structures

journal homepage: www.elsevier.com/locate/compstruct

Khalasa date palm leaf fiber as a potential reinforcement for polymeric composite materials

Elsadig Mahdi [a], Daniel R. Hernández Ochoa [b], Ashkan Vaziri [c], Aamir Dean [d], Murat Kucukvar [e]

[a] Department of Mechanical and Industrial Engineering, College of Engineering, Qatar University, P.O. Box 2713, Doha, Qatar
[b] Ministry of Municipality and Environment, Qatar, P.O. Box 22332, Doha, Qatar
[c] Mechanical and Industrial Engineering Department, Northeastern University, Boston, MA 02115, USA
[d] Institute of Structural Analysis (ISD), Leibniz Universität Hannover, Appelstr. 9A, 30167 Hannover, Germany
[e] Department of Mechanical and Industrial Engineering, College of Engineering, Qatar University, P.O. Box 2713, Doha, Qatar

ARTICLE INFO

Keywords:
Circular economy
Date palm fiber
Khalasa leaf
Fiber characterization
Morphology

ABSTRACT

The circular economy (CE) proposes a closed-loop supply chain-based production system and reduces the ecological systems' negative impacts. CE proposes a paradigm shift from a linear economy to a circular economy with the principles of 3Rs: reduce, reuse, and recycle. CE applications can be a viable option for the sustainable production of polymeric composite materials by decreasing the cost and improving product lifetimes and mechanical performance. This paper explores Khalasa date palm leaf fiber (KDPLF) as a reinforcement for polymeric composite materials. To this end, it is essential to examine their morphology, material properties, chemical composition, and water uptake. The investigated fiber was obtained from the Qatar University farm. The morphology examination was carried out using scanning electron microscopy. Thermogravimetric analysis has been used to examine the thermal stability of KDPLF. Morphological examination indicates that the lumen size for Khalasa is 32.8 ± 15.9 μm. The SEM morphology of the KDPLF cross-section showed high hemicellulose content. Tensile properties revealed that Khalasa fiber had tensile strength/tensile modulus of 47.99 ± 13.58 MPa and 2.1 ± 0.40 GPa, respectively. The results are also demonstrated that high variation in the mechanical properties and morphology was showed in KDPLF. Water uptake has significant effects on the properties of KDPLF/epoxy composite. Accordingly, as the moisture absorption of KDPLF/epoxy increases, its strength and stiffness decrease. As the moisture absorption of KDPLF/epoxy increases, its toughness increases.

1. Introduction

Global demand for resources is projected to double by 2050, and only 6% of materials are recycled globally [1]. The concept of a circular economy has become very popular since the world is expected to have inevitable supply shocks for scarce minerals and rare metals. Today, most of the countries aim to shift from a '*linear economy*' to a '*circular economy*' in which a closed-loop supply chain system will help the producers to become more resilient to the supply shocks, get benefit from the wasted materials, and reduce the environmental impacts related to the extraction of virgin raw materials [2]. The circular economy is based on the 3Rs: reduce, reuse, and recycle and proposes a closed-loop supply chain network. It significantly reduces the ecological systems' negative impacts by recirculating the products within the ecological system with the so-called 'cradle-to-cradle' thinking [3,4].

In response to a change of paradigm from a linear to a circular economy, which proposes the take-make-reuse type of system, several studies addressed the environmental benefits of circular business models. They also discussed its relevance with Sustainable Development Goals of the United Nations [5]. At a systemic level, circular economy applications will impact micro, meso, and macro systems and transform the regional, national, and global supply chains of production systems and reduce their overall environmental footprints globally. Furthermore, moving from a '*take-make-waste*' type of economy to '*take-make-recover*' eventually maintain, protect, transform, and strengthen the environment and will help reduce human health impacts through resource efficiency and improve human well-being through socio-economic benefits such as job creation, innovation in product design [6], and empowering the national economy with reduced dependencies to raw materials of other nations [7].

E-mail addresses: elsadigms@qu.edu.qa (E. Mahdi), dochoa@mme.gov.qa (Daniel R. Hernández Ochoa), a.dean@isd.uni-hannover.de (A. Dean), mkucukvar@qu.edu.qa (M. Kucukvar)

https://doi.org/10.1016/j.compstruct.2020.113501
Received 12 December 2020; Revised 12 December 2020; Accepted 16 December 2020
Available online 27 December 2020

Plant-based materials play a pivotal role in the transition to a circular economy. A circular economy approach can be a viable option for the sustainable production of polymeric composite materials by reducing their overall plastic content and increasing the product life cycles [8]. Today, agricultural production produces a massive amount of organic waste, which can undoubtedly play a transformative role in the circular economy for composite polymeric material production and foster recycled organic waste by minimizing waste being landfilled.

In the automotive application use of synthetic fibers, reinforced polymeric composites have dominated the energy absorber device [9–13]. The keen interest in using plant fibers as reinforcing materials seems to be a sustainable source to substitute synthetic fibers reinforced polymer composites [14]. Those fibers can produce competitive composites, enhance tensile and flexural resistance, and reduce costs and environmental pollution, among other advantages [15]. Many researchers have evaluated those fibers (such as hemp, jute, and albaca.) on their mechanical performance, relating it to morphology, composition, or water absorption [16]. Many ways have been designed to reduce such materials' hindrance and moisture absorption [17], usually changing surface roughness, polysaccharides content, or chemical groups. Therefore, it is crucial to know their physicochemical properties and mechanical behavior to determine the better way to use them as reinforcement [18].

Among the worldwide investigated fibers as reinforcement for composites is the date palm fiber. The date palm (Phoenix dactylifera) represents an essential source for economic and social life in Middle East countries. There are hundreds of date palm types used in almost all fields [19]. The palm produces natural fibers [20] used as promising materials for thermal and acoustic insulation. Some of the date palm fibers are used as an absorbent of different oils [21]. There are studies about the sugar composition of leaflets of date palm [22], the use of date palm stem fiber as reinforcement after alkali and acid treatment [18], the thermophysical and dielectric properties of the wood [19], the wood powder reinforcing a composite based on low-density polyethylene [23], the evaluation of the water uptake on the tensile behavior of natural fiber composites [16], and recently the structural and mechanical analysis of waste leaf sheath date palm fibers [24]. However, no reference was found in the literature related to the lumen (central void) dimensions of leaflets and their mechanical properties. This knowledge is required in order to promote the use of this waste material. The porosity and lumen size were important parameters that influenced natural fiber mechanical properties [18].

Natural fibers with small diameters improve the mechanical properties than larger ones [25,26]. The main mechanical properties of fiber reinforcement are specific strength and specific stiffness in the axial and transverse directions. In the axial direction, the reinforcement carries most of the load of the composite. The reinforcement is dominated by lumen size, microfibril angle, and cellulose content [27]. This high variability in tensile properties can be attributed to many reasons. According to Bodros [28], irregular cell, geometry, and fiber cross-sectional area are vital factors behind the variability in tensile properties. It is also well-known that natural plant fibers have a differing lumen, and only the cell-wall stands the tensile stress. It is interesting to note that fiber's diameter and lumen size are affected by each other. Shing-Chung Wong [29] stated that fibers with a large diameter result in a more considerable variation in the calculation of tensile properties. It is also found that along the fiber length, the cross-section shape is not regular. Therefore, the assumption of a uniform cross-section is significantly behind the significant variation of the tensile properties. Morphological examination showed that the fiber cells' age affects the cell's lumen size, which affects the uniformity of tensile properties.

On the other hand, the fiber's stiffness is significantly affected by the microfibril angle (MFA), and as the MFA increases, Young's moduli decrease [30,31]. V. Fiore [32] introduced Arundo donax L. fibers as a new candidate fiber-reinforced polymeric matrix. They investigated the mechanical properties and morphological of Arundo donax L. fibers. They used a mathematical formulation to study the effect of the fiber geometrical dimension on the mechanical properties. As part of a global trend concerning natural fibers' study, in this study, we used Khalasa date palm from Qatar, a country with abundant palm trees. After the extraction, treatment of Khalasa date palm fibers, the tensile properties were characterized, the tubular vessel dimensions were calculated, and the water absorption was measured.

2. Materials and methods

2.1. Materials

The Qatari Khalasa Date Palm Leaflet Fiber (KDPLF) is collected from Qatar University. Fig. 1a, 1b, and 1c show the green date palm, dried date palm leaflet, and continuous date palm leaflet fibers. The KDPLF bundles were extracted from stems and well-kept in plastic. All collected samples were immersed in water for washing, shredded into fiber bundles, and dried at room temperature (27 °C). Then, long fibers extracted using a carefully designed needle brush. The chemical composition of raw date palm fiber (KDPLF) is affected by its origin and agricultural parameters. For Khalasa, cellulose represents 47.14% of its weight, amount of lignin (36.73%), and hemicellulose (16.13%). It is essential to know the fibers' density to predict the mechanical properties of the fiber-reinforced composite. Accordingly, Khalasa fibers density was measured for five samples by a densitometer and found to be 1.233 g/cm^3.

Epoxy resin A-B was purchased from Yestar Conductive Material Co., Ltd (A: resin, B: hardener). Five parts by weight of epoxide resin mixed with 1 part by weight of hardener. Based on the manufacturer's recommendation, the density of A = 1.12 ± 0.1 g/cm^3, B = 0.8 ± 0.1 g/cm^3, Young's modulus of 3.35 GPa, and Poisson's ratio of 0.35.

2.2. Methods

The scanning electron microscopy (SEM) was used to examine the fiber morphology. The morphology examination process was carried out using a Nova Nano SEM 450 FEI, in which each fiber was prepared by cutting them to a height of 10 mm, coated with gold. As stated earlier, natural plant fibers exhibited variation in dimensions along their longitudinal direction. The examined fibers show irregular shapes and non-uniform cross-sections.

The KPDLF cellulose content was computed by utilizing the density method [33]. The density method determines the cellulose content of KPDLF by evaluating an apparent and the real density with the pycnometer helium technique and the Archimedes process using benzene with a density of 0.875 g/cm^3, respectively. However, for measuring the bulk density of KPDLF, benzene was used as a nonpolar solvent. Samples of KPDLF were first weighed in the atmosphere, and again dipped in benzene, and reweighted. To determine the KPDLF apparent density (ρ_A), one can utilize the following equation:

$$\rho_{KPDLF} = \frac{\rho_b \times W_{fa}}{W_{fa} - W_{fb}} \quad (1)$$

Where

ρ_b is the benzene density;

W_{fa} and W_{fb} are the fibers weights in air and benzene, respectively.

The KPDLF's heat capacity was recorded using Differential scanning calorimetry (DSC 8500:Perkin Elmer thermogravimetric analyzer) at a heating rate of 10°/min at the nitrogen media from room temperature up to 700 °C. The average of the five samples was recorded. The investigation of the effect of the moisture content on KDPLF and KDPLF/epoxy properties has been carried out; ten samples for each time inter-

Fig. 1. (a) Green date palm (b) Dried date palm leaflet (c) Continuous Date palm leaflet fibers.

val were immersed in water. KDPLF's moisture content has been analyzed using Fick's diffusion. Accordingly, all KDPLF/epoxy specimens were dried in a furnace at 50 °C and cool to room temperature. The drying process was repeated until the readings of the specimen's mass have converged. Water uptake was examined by immersing the KDPLF/Epoxy samples in a water tank at 23 °C for a different period of intervals. Then, the immersed specimens were taken out and dried with a cloth. The specimens' weights were measured within 1 min of their removal from water. The immersion time intervals were 2, 4, 6, 12, 24, and 48 up to 72 h. A universal testing machine (INSTRON 5943, Northeastern University, USA) was used to determine the tensile properties of the KDPLF, according to D3822/D3822M [34] with a load-carrying capacity of 1 kN. Fibers were measured in-depth and width at least at ten different points along their length, and an average cross-section was calculated for each sample. A pair of custom-designed grips (Fig 2aia) was manufactured to perform tensile tests on the fibers. These grips were printed on a 3D printer machine (Eden 260 V, Stratasys Ltd., Eden Prairie, MN, USA) with Acrylonitrile Butadiene Styrene (ABS). Fig 2bib shows the grips and alignment to ensure accurate, repeatable results. The machine cross-head speed of 1.5 mm/min was used for the tensile test. Five specimens were tested for each variety. A compression molding machine was used to produce KDPLF/Epoxy composite specimens for tensile test. Specimens were prepared

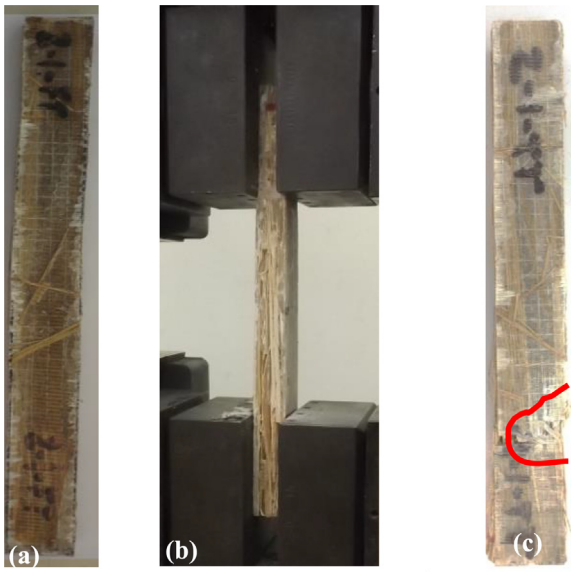

Fig. 2b. (a) Rectangular KPDLF/epoxy , (b) Experimental setup (c) Fractured Speciemn.

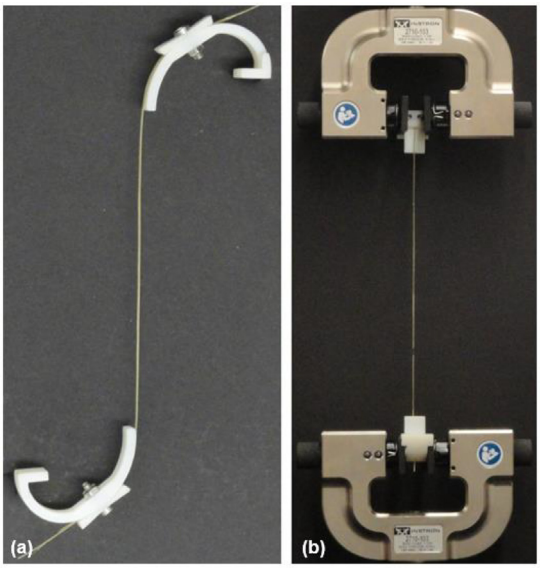

Fig. 2a. Tensile test setup: (a) Costume ABS designed grips, (b) Experimental setup.

per D3039/D3039M [35] rectangular shape specimens, as shown in Fig. 1b. Accordingly, five specimens with a constant rectangular cross-section were tested at a machine cross-head speed of 2 mm/minute. The gauge length of the specimens was 60 mm, and the thickness was 2 mm.

3. Results and discussion

3.1. Physical and chemical properties

The Khalasa date palm fibers' real density (ρ_r) is determined using a gas pycnometer found to be 1.233 g/cm^3. On the other hand, the Khalasa date palm fibers' bulk density is measured using the density method and determined to be 0.893 g/cm^3. On the other hand, the obtained value of the Khalasa date palm fibers' cellulose content was computed using Eq. (1), which is equal to 43.59%. The contents of cellulose, hemicellulose, lignin (ASTM D1106–96), and ash (ASTM E1755–01) in Khalasa date palm fibers have been determined using methods that were suggested by Saura-Calixto [36]. Table 1, one can note that the lignin content of Khalasa fiber is the second highest after the coir fiber, while its hemicellulose content is also the second-highest after Arundo fiber. Furthermore, the cellulose content of Khalasa fibers is in the medium range compared to the other fibers.

Table 1
Properties and Composition of Khalasa fibers and some natural fibers from literature.

Fiber Type	Cellulose %wt	Hemi-cellulose %wt	Lignin %wt	Ash %wt	T_{onset} ○C	Density g/cm3	Max Strength MPa	Elongation at Break %	Tensile Modulus GPa
Khalasa	47.14	16.13	34.77	1.96	341	1.233	47.99	1.89	2.10
Coir	43.00	0.30	45.00	–	–	1.200	175	5.0	30.00
Cotton	85–90	5.70	–	–	–	1.550	287–597	5.50–12.60	7.00–8.00
Arundo	43.20	20.50	17.20	1.90	275	1.168	248	9.40	3.24
Ferula	53.30	8.50	1.40	7.00	200	1.240	475	52.70	4.20

3.2. Thermal analysis

The thermogravimetric analysis (TGA) of khalasa date palm fiber is shown in Fig. 3. It is quite clear that decomposition temperatures of KPDLF were found to have excellent thermal stability at 341 ˚C. The relationship between the temperature and weight loss curve can be divided into four stages. The first stage is from 40 to 120 ˚C, is associated with an insignificant loss in weight. The thermogravimetric analysis (TGA) of khalasa date palm fiber is shown in Fig. 3. It is quite clear that decomposition temperatures of KPDLF were found to have excellent thermal stability at 341 ˚C. The relationship between the temperature and weight loss curve can be divided into four stages. The first stage is associated with an insignificant loss in weight attributed to the evaporation process. The second stage is between 120 ˚C and 325 ˚C, where the cellulosic substances are degraded. On the other hand, the degradation process of noncellulosic components occurred during the third stage at the temperature (325 ˚C–450 ˚C). In the fourth stage, an insignificant weight loss was observed.

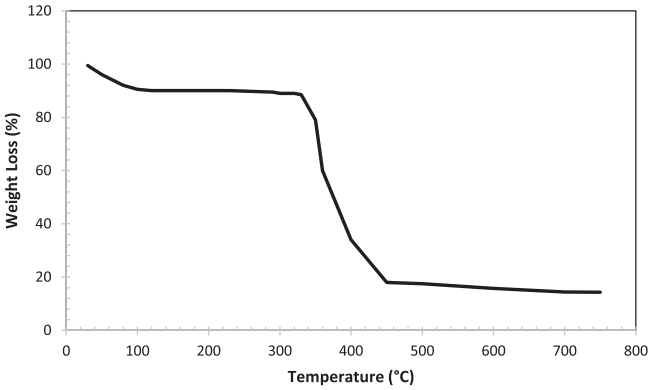

Fig. 3. TG curve of KPDFL Fibers.

3.3. Morphology characterization

The surface morphology of the date palm fiber was analyzed using SEM. The SEM micrographs of KDPLF and KDPLF/epoxy are shown in Figs. 4, 5, 8–10. Fig. 5 shows the cell wall's microstructures in dry conditions and the cell wall biodegradation due to 48 h of underwater absorption for KDPLF continuous tubular vessel morphology. Based on the fact that the lumen size influences the water uptake, and thus, the moisture content [37,38], larger lumen structures made the fiber uptake more water. KDPLF, the same as natural fibers derived from plants, consists mainly of cellulose fibrils embedded in the lignin matrix. It is also clear that KDPLF itself is a layered composite structure composed of three cell walls with different thickness (see Fig 4ai). As stated in the literature, the mechanical properties of KDPLF are affected by the morphology of the secondary cell walls, in which the thick middle layer is located. The thick middle layer is composed of cellulosic molecules (i.e., hemicelluloses and lignin). As mentioned earlier, the KPDLF is composite, where the lignin-hemicelluloses play the matrix role, while the microfibrils play the role of the reinforcement. The structural components in KDPLF were found to be similar to many natural plant fibers are cellulose, hemicellulose, pectin, lignin, and wax. Fig 4bi and 4bii show the SEM micrographs of Khalasa date palm fiber/epoxy and tensile test specimen, respectively. The KDPLF cellulosic contents are observed to be composed of crystalline microfibrils, longitudinally aligned along the fiber axis, as shown in Fig 4ai.

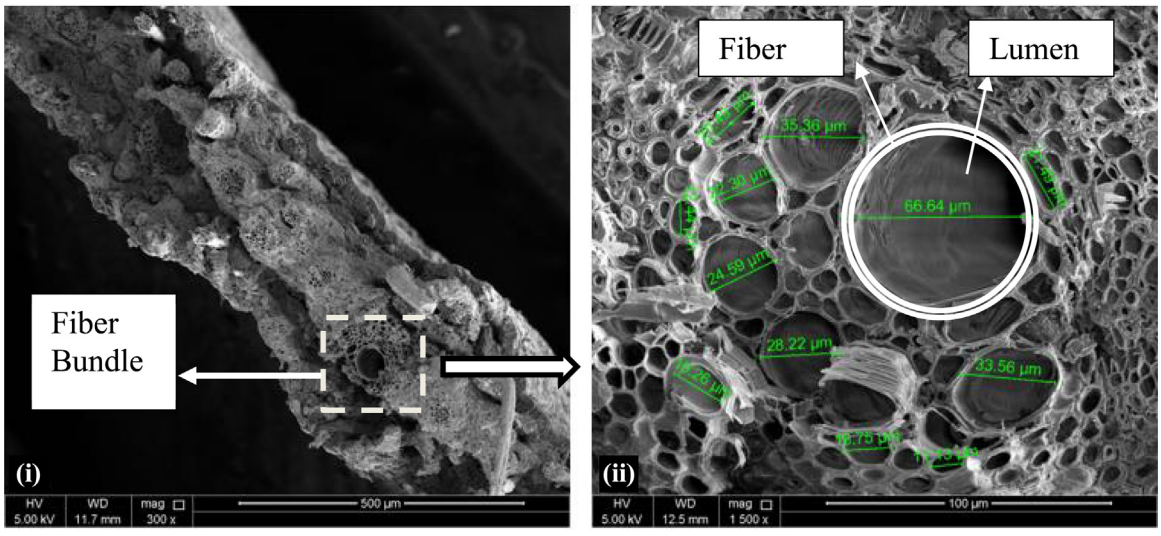

Fig. 4a. SEM micrographs of Khalasa date palm fiber: (i) leaflet morphology and (ii) continuous tubular vessel dimensions.

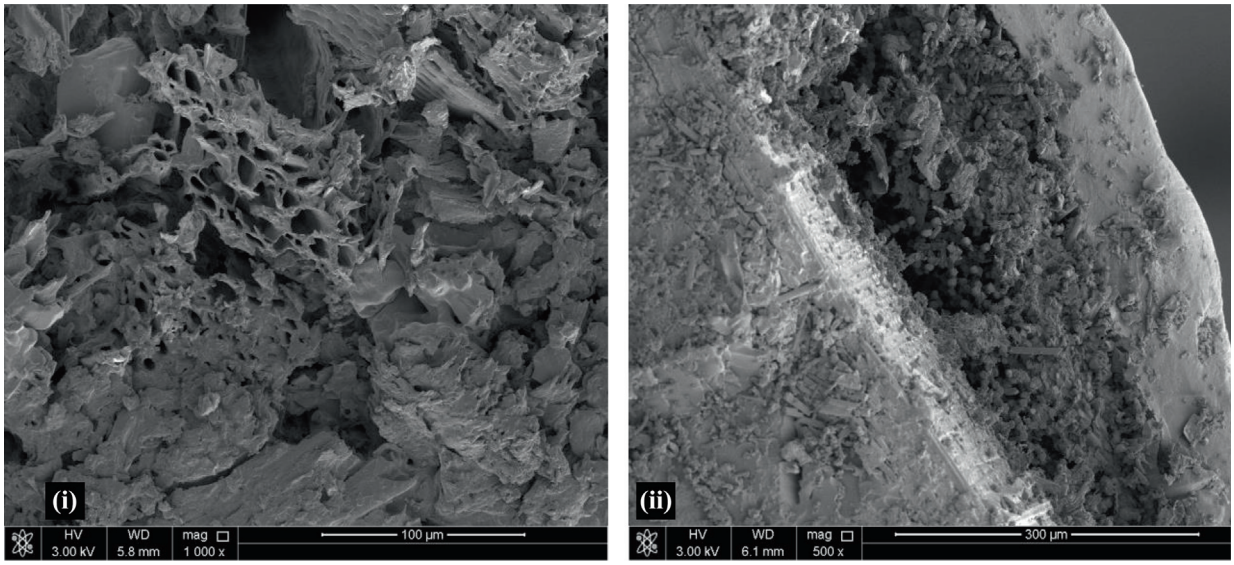

Fig. 4b. SEM micrographs of (i) Khalasa date palm fiber/epoxy and (ii) Tensile test specimen.

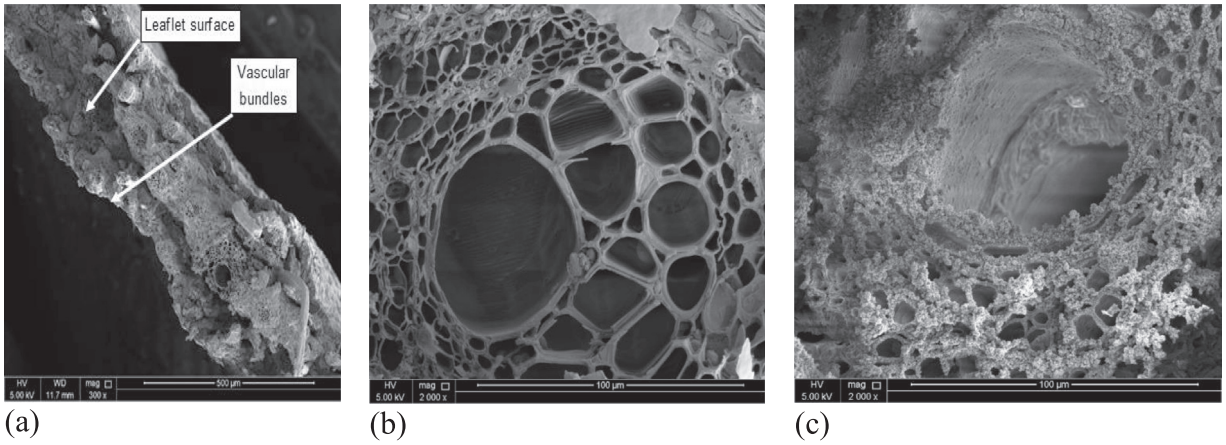

Fig. 5. (a) Khalasa DPLF vascular bundles morphology. (b) cell wall in dry conditions. (c) cell wall biodegradation due 24 h under moisture absorption.

The observed lignin, also known as a complex hydrocarbon polymer, is believed to give KPDLF rigidity and ease water uptake. It is essential to mention that voids are also present in KDPLF natural fibers, which indicates a certain degree of porosity. It is well-known that porosity promotes higher moisture absorption of fiber. The water uptake was determined by the weight difference before immersion and after immersion. The percentage of weight gain was computed at various time intervals, and the water uptake versus immersion time was plotted, as shown in Fig. 6. Natural plant fiber-based composites have limitations in outdoor applications as compared to synthetic fibers based composites. The limitations are due to its water uptake because of higher hemicellulose contents. Accordingly, KDPLF absorbs more moisture and experience swelling and dimensional increase. From all the various parts of the date palm, leaflets had the highest amounts of extractives and protein, 24% and 10%, respectively. It is important to note that natural fibers' moisture content is attributed to the hemicellulosic plant cell wall. Higher water uptake eases the microbial attack. Fig. 5b shows the KDPLF vascular bundle cell-wall biodegradation morphology due 24 h under moisture absorption. Herein, the diffusion coefficient is proportional to the concentration gradient of this substance. The diffusion coefficient indicates that the material migrates through a unit surface in a unit time at a concentration gradient of unity. The high content of hemicellulose and pores in the leaflets connective tissue facilitates the moisture absorption process. The KDPLF showed high hydrophilic behavior and reach 98.4% saturation water uptake in 24 h (see Fig. 6).

3.4. Tensile behavior

Moisture fiber content influences the degree of crystallinity, crystalline orientation, tensile strength, swelling behavior, and porosity of fibers. Twenty-five fibers were selected randomly to appreciate the effect of moisture content on the tensile behavior of KDPLF. Young's moduli, ultimate tensile strength, and elongation at break were calculated from the stress–strain curve for KDPLF. Table 1ists the composition and properties of Khalasa fibers and some natural fibers from literature. As shown in Table 1, one can note that the lignin content of Khalasa fiber is the second highest after the coir fiber, while its hemicellulose content is also the second-highest after Arundo fiber. One can note that the cellulose content of Khalasa fibers is in the medium range compared to the other fibers. Table 2 gives the tensile properties of KDPLF before and after soaked in water, respectively. The

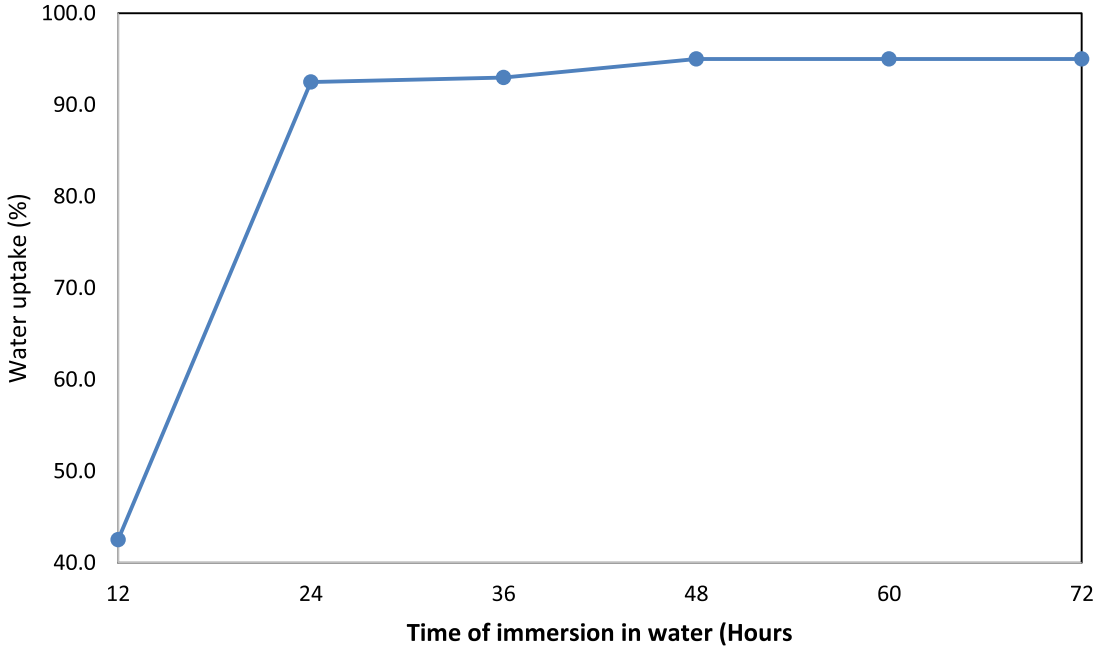

Fig. 6. Khalasa DPLF moisture absorption.

Table 2
Tensile properties of KDPLF before and after soaked in water.

	Dry Condition	Under Water Absorption
Tensile strength (MPa)	47.99 ± 13.58	38.16 ± 15.67
Modulus (GPa)	2.10 ± 0.40	1.41 ± 0.45
Elongation (%)	1.89 ± 0.41	2.45 ± 0.22

variability in the reported properties is probably attributed to the possible residual stresses and damage during the fibers' extraction process.

3.5. The water uptake behavior of KDPLF /Epoxy composite

The water uptake in the KDPLF/Epoxy Composite was computed by the difference in weight between the dry and the wet samples using the following and mechanical properties of the fibers used:

$$c = \frac{m_2 - m_1}{m_1} \times 100 \tag{2}$$

Where;

c is the percentage change in mass relative to the initial mass,

m_1 and m_2 are the specimen's masses before and during aging, respectively.

For one-dimensional water uptake, both sides of each specimen are exposed to the same environment; the total water uptake c(t) can be formulated as found in ISO62:2008 [39] as follows:

$$c(t) = c_s - c_s \frac{8}{\pi^2} \sum_{k-1}^{20} \frac{1}{(2k-1)^2} exp\left[-\frac{(2k-1)^2 D\pi^2}{d^2} t\right] \tag{3}$$

Where;

c_s is the water absorption at saturation,

k is the summation index,

d is the thickness,

t is the time and

D is the mass diffusivity in KDPLF/Epoxy.

Fick's law has been used to describe the composite material's diffusion properties and determined by weight gain of pre-dried specimens immersed in water by using the following equation:

$$\sqrt{D} = \frac{1}{c_s} \cdot \frac{d}{0.52\pi} \cdot \frac{c(t)}{\sqrt{t}} \tag{4}$$

Fig. 7a shows the percentage of weight vs. time for the KDPLF/Epoxy composite. On the other hand, the tensile stress–strain curves for the KDPLF/Epoxy composite before and after soaked in water are shown in Fig. 7b. The water uptake process for KDPLF and KDPLF composites is linear initially, then slows and approaches saturation 24 h. The water uptake by KDPLF was computed to be 94.93% more than the KDPLF composite. The diffusion coefficient for KDPLF/Epoxy composite diffusion coefficient was determined to be $4.17 \cdot 10^{-3}$ m2/s. It can be seen that the water uptake significantly decreased in the case of KPDLF/epoxy composite because the epoxy resin partially fills the KPDLF's lumen. The resin filling the lumen structures blocked the water channels, which is considered an essential mechanism for the moisture absorption of plant-reinforced composites. It is observed that KDPLF swells when it is composite is exposed to moisture. The fiber swelling promotes micro-cracking in the epoxy matrix, as shown in Figs. 8-10. The content of hemicellulose dominated the moisture con-

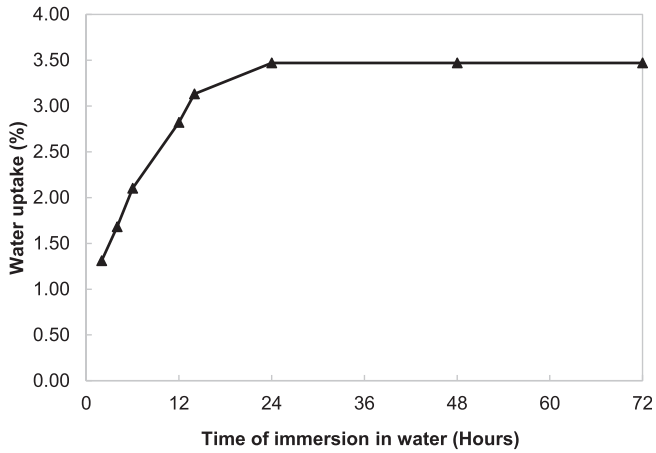

Fig. 7a. KDPLF/Epoxy moisture absorption.

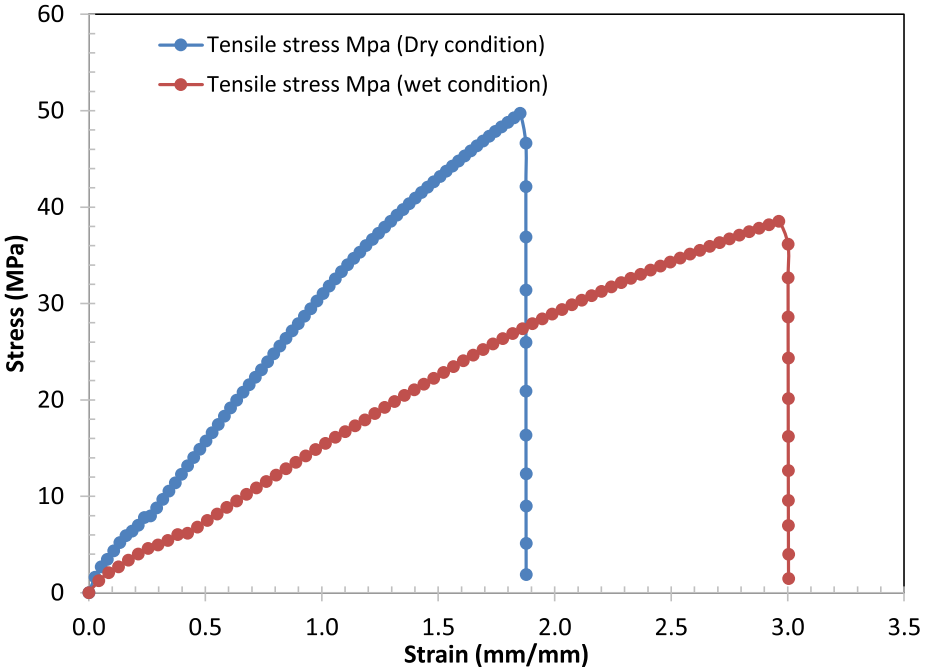

Fig. 7b. Stress–strain curve of KPDFL/epoxy composite.

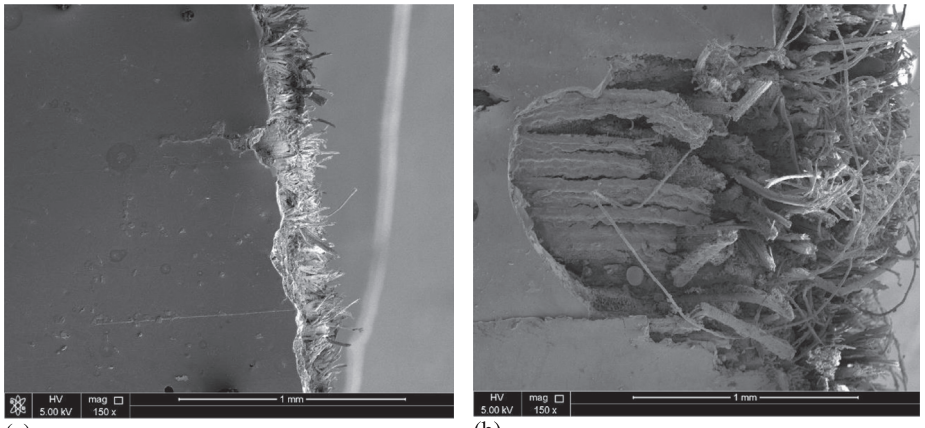

Fig. 8. KDPLF/Epoxy moisture expansion damage (a) matrix crack in dry conditions, (b) fiber–matrix debonding, crack development, fiber swelling, and loss of matrix particles due 24 h under moisture absorption.

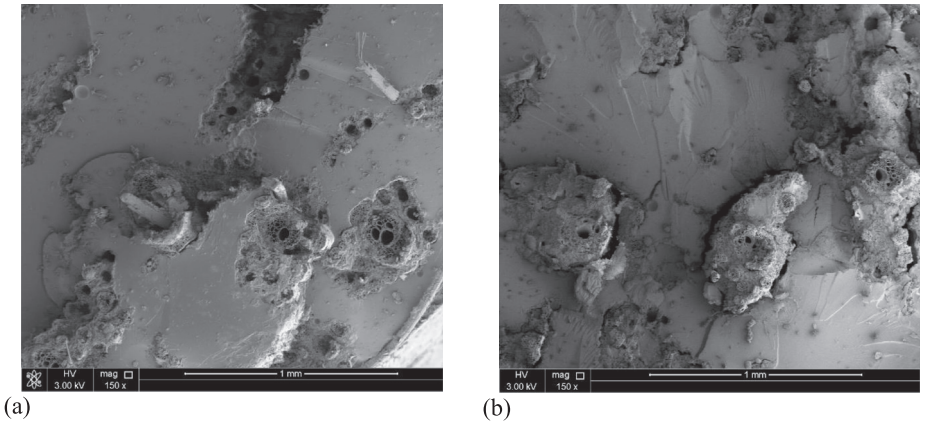

Fig. 9. Morphology of damaged KDPLF/Epoxy (a) debonding, fiber fracture, fiber pull out under dry conditions, (b) fiber swelling, fiber pull out, debonding increase, and matrix crack due 24 h under moisture absorption.

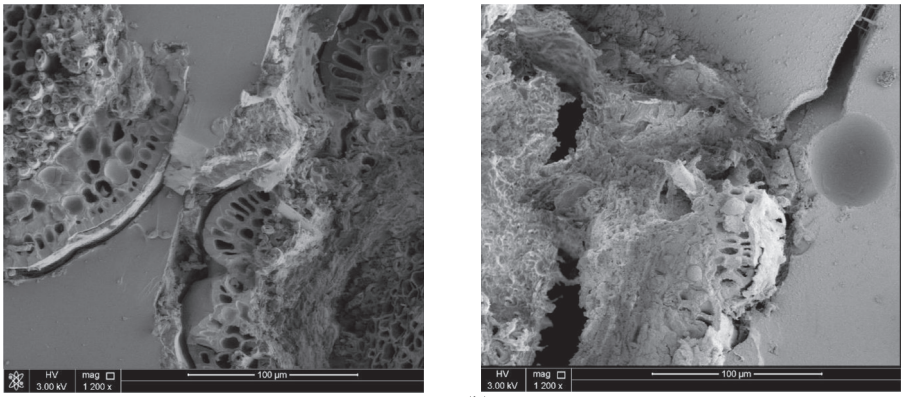

Fig. 10. Morphology of damaged KDPLF/Epoxy (a) fiber pull out and fiber fracture, fiber–matrix debonding under dry conditions, (b) matrix crack, fiber swelling, debonding due to the fiber swelling stress, and fiber biodegradation due to attack by water molecules under 24 h moisture absorption.

tent in natural fiber composites. As the content of hemicellulose increases, the moisture content increases. Based on the previous study, the hemicellulose content in KDPLF is in the range of 26–28%.

The hemicellulose content is believed behind the more water absorption into the interface between the fiber and matrix, generating volumetric (swelling) stress leading to KDPLF composite failure. The failure mode was observed to be a debonding between fiber and matrix. The development of osmotic pressure pockets initiates the debonding failure mechanism at the fibers' surface due to water molecules' diffusion. Fig. 10a shows that KDPLF/Epoxy has only experienced matrix cracking in dry conditions. On the other hand, Fig. 10b shows fiber–matrix debonding, crack development, fiber swelling, and matrix crack to affect moisture content. Table 2 presents the coefficients of moisture expansion for the KDPLF/Epoxy composite. However, moisture absorption produces dimensional changes in the material due to the matrix and fiber swelling; the resulting volumetric strain can be computed as:

$$\varepsilon_m = \beta \cdot M \tag{5}$$

Where; ε_m is the volumetric strain due to moisture absorption, M is the moisture content at the time (t), and β is the coefficient of moisture expansion (CME) computed as:

$$\beta = \frac{\Delta l}{l_0} / \frac{\Delta m}{m_0} \tag{6}$$

Where;

β is the coefficient, l_0, m_0 initial length and mass respectively, and Δl, Δm time depends on length/mass variation. Table 3 gives the coefficient of moisture expansion.

KDPLF/Epoxy composites shown different damage morphology for dry and water immersed (exposure time 24 h). The SEM photographs show fiber fracture in the fiber–matrix coupling area, and fiber pulls out in the fiber core as the primary damage characteristics. It is also evident that the KDPLF fiber core area has a high degree of porosity (vascular bundles). This porosity promotes higher moisture absorption of fiber by capillarity along the fiber core/coupling area and coupling area/matrix interface. Debonding between the fiber core and the fiber–matrix coupling area reduced the composite stress transfer capacity. In a polymeric composite, the water-uptake can be occurred by three mechanisms: by imperfections within the matrix (pores and cracks) matrix, by diffusion inside the, or by capillarity and the fiber/-matrix interface. Water uptake in polymeric composites involves molecules of free and trapped water. The water uptake process in plant fiber-reinforced composite materials consists of some stages. During the first stage, free water molecules enter and rest inside the fibers, namely the hydrophilic groups, affecting the interfacial strength between the plant fibers and the polymeric matrix. The affected interfacial strength leads to material degradation, and matrix cracking around swollen fibers has been observed. The cracks in the matrix increase water uptake. The development of osmotic pressure pockets initiates debonding between fiber and matrix at the fibers' surface due to the leaching of water-soluble substances from the fiber surface. KDPLF/ epoxy composite tensile test damage characteristics under 24 h of moisture absorption showed different damage morphology: micro-cracks in the matrix, fiber swelling, fiber biodegradation, debonding between the fiber core and the fiber–matrix coupling area due to the fiber swelling stress, and fiber pull out in the fiber core.

As mentioned earlier, natural plant fiber-reinforced composites suffer from their high water uptake capability because it degrades their

Table 3
Coefficient of moisture expansion.

CME	%	Direction
β_1	0.362983	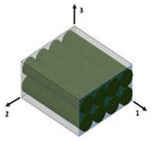
β_2	0.541918	
β_3	2.792627	

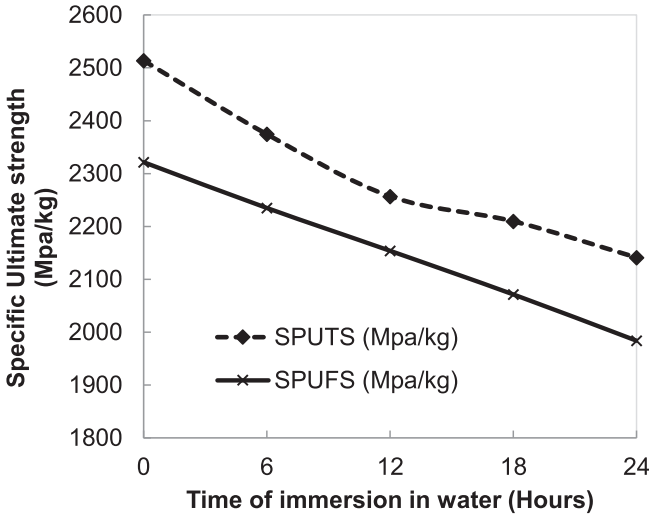

Fig. 11. KDPLF/Epoxy specific ultimate strength.

mechanical properties. This degradation was found to be due to the low-stress transfer at the interface between the fiber–matrix. Fig. 11 shows the effect of moisture absorption on the specific ultimate strength of KDPLF composites. The specific ultimate tensile strength drops sharply as the moisture uptake percentage increases. Both the tensile strain increases as the moisture uptake percentage increases. The computed results showed that the tensile strain increased by 1.2%, respectively. This decrease in KDPLF composites' strength is attributed to water's plasticization effect, weakening the fiber/matrix interface. Instantly, a significant change in hemicellulose's microstructure was observed. Fig. 8a and 8b show the microstructure for KDPLF composites before and after water uptake. This change in microstructure is believed to increase the ductility of KDPLF composites due to the moisture content. However, empirical equations that relate the KDPLF composites' specific strengths with the immersion time have extracted using the best fitting curve model. The polynomial relationship with R-square value 0.99 between KDPLF/Epoxy composites' specific ultimate tensile strength (SPUTS) and immersion time (t) is

$$SPUTS = -0.0166t^3 + 1.0174t^2 - 30.394t + 2515.7 \quad (7)$$

Also, the linear relationship with R-square value 0.99 for (SPUFS) and immersion time (t) is

$$SPUFS = -13.987t + 2321 \quad (8)$$

These equations are valid for up to 24 h because, after this time, the composite reaches its moisture content saturation. Fig. 12 shows the moisture absorption influence in the specific modulus. The specific modulus decreases as the moisture content increases. Accordingly, the elastic modulus of the composite is reinforcement dominant, in which moisture content has been found to have a significant effect on composite stiffness. The KDPLF/Epoxy composite shown stress transfer capability reduction between fiber and matrix due to moisture content. The water uptake is less critical for the flexural failure mode than in the tensile failure mode. This observation is because the flexural samples fail in the combination of compression, shear, and tension mode. Empirical equations that relate the DPLF composites' specific moduli with the immersion time have extracted using the best fitting curve model. The lineal relationship with an R-square value of 0.99 between DPLF/Epoxy composites' specific tensile moduli (SPTM) and immersion time (t) is

$$SPTM = -1.961t + 265.65$$

Also, the polynomial relationship with R-square value 0.99 for (SPFM) and immersion time (t) is

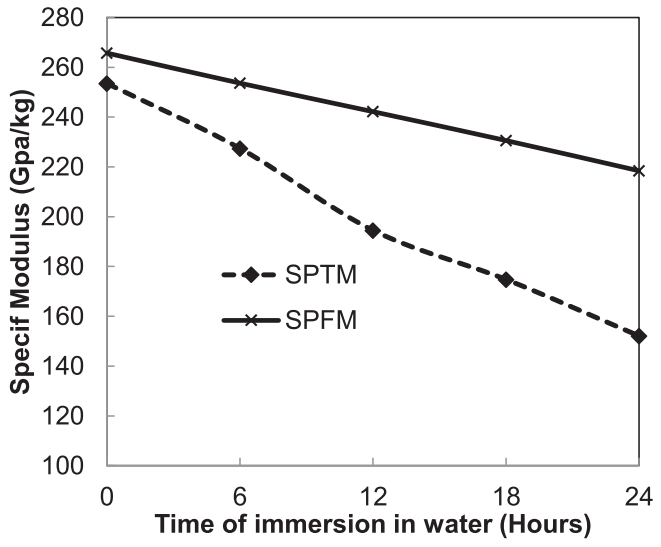

Fig. 12. KDPLF/Epoxy specific modulus.

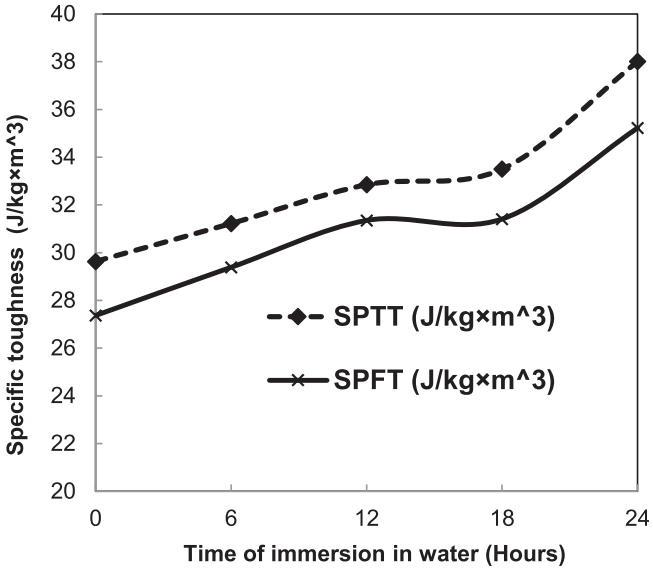

Fig. 13. KDPLF/Epoxy specific toughness.

$$SPFM = 0.0015t^3 - 0.0142t^2 - 4.7465t + 253.98 \quad (10)$$

These equations are valid for up to 24 h because after this time, the composite reaches its moisture content saturation, and no more change was observed.

Fig. 13 shows that the specific toughness under moisture conditions increases. The KDPLF/Epoxy with high moisture content is less brittle and requires more energy to break it; the plasticization effect of water, water pockets, hemicellulose degradation, fiber swelling, debonding, and moisture expansion effect have an important influence on the material toughness. The empirical equations which relate the DPLF composites' specific toughness with the immersion time have extracted using the best fitting curve model. The polynomial relationship with R-square value 0.97 between DPLF/Epoxy composites' specific tensile moduli (SPTT) and immersion time (t) is

$$SPTT = 0.0015t^3 - 0.0433t^2 + 0.541t + 29.55 \quad (11)$$

Also, the polynomial relationship with R-square value 0.95 for (SPFM) and immersion time (t) is

$$SPFM = 0.0015t^3 - 0.0496t^2 + 0.6705t + 27.262 \quad (12)$$

These equations are valid for up to 24 h because after this time, the composite reaches its moisture content saturation, and no more change was observed.

4. Conclusions

This paper introduces Khalasa date palm leaf fiber (KDPLF) as a reinforcement for polymeric composite materials. Similar to other natural fibers, high variation in the mechanical properties and morphology was showed in Khalasa fibers. The investigation findings revealed that the morphological properties indicate the lumen size for KDPLF (32.8 ± 15.9) μm, while KDPLF's cross-section showed high hemicellulose content. Moreover, the effect of water absorption has been found to have significant effects on the mechanical properties of date palm leaf fiber reinforced epoxy composite. Accordingly, as the moisture content increases, Young's modulus, the tensile strengths of KDPLF/epoxy composites decrease. On the other hand, as the moisture content increases, Khalasa /epoxy composites' toughness increases.

This paper examined the morphology, material properties, chemical composition, and water uptake of Khalasa date palm leaf fiber.

For future research, the authors propose to develop a holistic life-cycle sustainability assessment model in which the social, economic, and environmental performance of KDPLF will be assessed from the cradle to the grave, and the life cycle sustainability performance of KDPLSs will be compared with other natural composites. The researchers also aim to build global and hybrid life cycle assessment models to reveal the regional direct and global indirect environmental benefits such as carbon footprint reduction, water use reduction, and waste minimization of a circular economy application with KDPLF and synthetic fibers. Multi-regional hybrid life cycle assessment models will serve as the best to investigate the micro and macro-level benefits of using organic waste materials as a reinforcement to polymeric products considering various macroeconomic factors such as contribution to national gross domestic production, employment, job creation through recycling sector, and improved health and well-being impacts related to producing petrochemical-based polymeric products [40,41]. Finally, several multicriteria decision-making models such as fuzzy sets theory and expert judgment-based multi-attribute decision-making algorithms can also be used to extend the scope of the current researcher to select the most sustainable business models considering not only mechanical performance but also environmental, cost, and well-being of the society, simultaneously and integrated multicriteria decision-making model with life cycle sustainability assessment model can be found in the literature [42].

Declaration of Competing Interest

The authors declare that they have no known competing financial interests or personal relationships that could have appeared to influence the work reported in this paper.

Acknowledgment

The authors would like to acknowledge the financial support of the Qatar National Research Fund (a part of the Qatar Foundation) through the National Priorities Research Program NPRP 5-068-2-024.

References

[1] Haas W, Krausmann F, Wiedenhofer D, Heinz M. How circular is the global economy?: An assessment of material flows, waste production, and recycling in the European Union and the world in 2005. J Ind Ecol 2015:1–13.
[2] Korhonen J, Honkasalo A, Seppälä J. Circular economy: the concept and its limitations. Ecol Econ 2018;143:37–46.
[3] Geissdoerfer M, Morioka SN, de Carvalho MM, Evans S. Business models and supply chains for the circular economy. J Cleaner Prod 2018;190:712–21.
[4] Kirchherr J, Reike D, Hekkert M. Conceptualizing the circular economy: An analysis of 114 definitions. Resour Conserv Recycl 2017:221–32.
[5] Ghisellini P, Cialani C, Ulgiati S. A review on circular economy: the expected transition to a balanced interplay of environmental and economic systems. J Cleaner Prod 2016;114:11–32.
[6] Stahel WR. The Circular Economy. Nature 2016;531(7595):435–8.
[7] Merli R, Preziosi M, Acampora A. How do scholars approach the circular economy? A systematic literature review. J Cleaner Prod 2018;178:703–22.
[8] Shogren, R, D Wood, W Orts, and G Glenn. 2019. “Plant-based materials and transitioning to a circular economy.” Sustainable Production and Consumption of 194-215.
[9] Badie MA, Mahdi E, Hamouda AMS. An investigation into hybrid carbon/glass fiber reinforced epoxy composite automotive driveshaft. Mater Des 2011;32 (3):1485–500.
[10] Mahdi E, Alkoles OMS, Hamouda AMS, Sahari BB, Yonus R, Goudah G. Light composite elliptic springs for vehicle suspension. Compos Struct 2006;75(1-4):24–8.
[11] Mahdi E, Sebaey TA. Crushing behavior of hybrid hexagonal/octagonal cellular composite system: Aramid/carbon hybrid composite. Mater Des 2014;63:6–13.
[12] Mahdi E, Hamouda AMS. An experimental investigation into mechanical behavior of hybrid and nonhybrid composite semi-elliptical springs. Mater Des 2013;52:504–13.
[13] Mahdi, E., Sahari, B.B, Hamouda, A.M.S., Khalid. Y.A., “An experimental investigation into crushing behavior of filament-wound laminated cone–cone intersection composite shell, Composite .” Composite Structures 7. E Mahdi, B.B Sahari, A.M.S Hamouda, Y.A Khalid, An experimental investigation into crushing behavior of filament-wound laminated cone–cone intersection composite shell, Composite StructuresVolume 51, Issue 3, March 2001; 2001 p. 211-19.
[14] Faruk O, Bledzki AK, Fink H-P, Sain M. Biocomposites reinforced with natural fibers.“ 8. Faruk, O., Bledzki, A. K., Fink, H.-P., and Sain, M. (2012). ”Biocomposites reinforced with natural fibers: 2000–2010. Prog Polym Sci 2012;37(11):1552–96. https://doi.org/10.1016/j.progpolymsci.2012.04.003 1552-1596.
[15] Senwitz C, Kempe A, Neinhuis C, Mandombe J, Branquima M, Lautenschlager T. Almost forgotten resources – biomechanical properties od traditionally used bast fibers from Northern Angola. BioResources 2016:7595–607.
[16] Mahdi E, Hernández DR, Eltai EO. Effect of water absorption on the mechanical properties of long date palm leaf fiber reinforced epoxy composites. J Biobased Mater Bioenergy 2015;9(2):173–81.
[17] Sbiai A, Kaddami H, Sautereau H, Maazouz A, Fleury E. TEMPO-mediated oxidation of lignocellulosic fibers from date palm leaves. Carbohyd Polym 2011:1445–50.
[18] Alawar A, Hamed AM, Al-Kaabi K. Characterization of treated date palm tree fiber as composite reinforcement. Compos Part B 2009;40(7):601–6.
[19] Agoudjil B, Benchabane A, Boudenne A, Ibos L, Fois M. Renewable materials to reduce building heat loss: Characterization of date palm wood. Energy Build 2011;43(2-3):491–7.
[20] AlMaadeed MA, Nógellová Z, Mičušík M, Novák I, Krupa I. Mechanical, sorption, and adhesive properties of composites based on low-density polyethylene filled with date palm wood powder. Mater Des 2014:29–37.
[21] Abdelwahab O, Nasr SM, Thabet WM. Palm fibers and modified palm fibers adsorbents for different oils. Alexand Eng J 2017;56(4):749–55.
[22] Bendahou A, Dufresne A, Kaddami H, Habibi Y. Isolation and structural characterization of hemicelluloses from the palm of Phoenix dactylifera L. Carbohyd Polym 2007:601–8.
[23] AlMaadeed MA, Kahraman R, Noorunnisa P, Madi N. Date palm wood flour/glass fiber reinforced hybrid composites of recycled polypropylene: Mechanical and thermal properties. Mater Des 2012:289–94.
[24] Bourmoud A, Dhakal H, Habrant A, Padovani J, Siniscalco D, Ramage M, et al. Exploring the potential of waste leaf sheath date palm fibers for composite reinforcement through structural and mechanical analysis. Composites A 2017:292–303.
[25] Shalwan A, Yousif BF. Investigation on interfacial adhesion of date palm/epoxy using fragmentation technique. Mater Des 2014;53:928–37.
[26] Placet, V., Trivaudey, F., Cisse, O., Gucheret-Retel, V., Boubakar, M. L., Diameter dependence of the apparent tensile modulus of hemp fibers: A morphological, structural or ultrastructural effect? Compos Part A-Appl Sci Manuf ; 2012: 275–87.
[27] dDjafari, S.R., “Physical and Mechanical properties of natural fibers.” In: Advanced High Strength Natural Fibre Composites in Construction, by Mizi Fan and Feng Fu, 87-114. Elsevier; 2017.
[28] Bodros E, Baley C. Study of the tensile properties of stinging nettle fibers (Urtica dioica). Mater Lett 2008:2143–5.
[29] Wong Shing-Chung, Baji Avinash, Leng Siwei. Effect of fiber diameter on tensile properties of electrospun poly(ε-caprolactone). Polymer 2008;49(21):4713–22.
[30] Lichtenegger H, Reiterer A, Stanzl-Tschegg SE, Fratzl P. Variation of Cellulose Microfibril Angles in Softwoods and Hardwoods-A Possible Strategy of Mechanical Optimization. J Struct Biol 1999;128(3):257–69.
[31] Gassan J, Chate A, Bledzki A. Calculation of elastic properties of natural fibers. J Mater Sci 2001:3715–20.
[32] Fiore V, Scalici T, Valenza A. Characterization of a new natural fiber Arundo donax L. as potential reinforcement of polymer composites. Carbohydr Polym 2014:77–83.
[33] Mwaikambo LY, Ansell MP. The determination of porosity and cellulose content of plant fibers by density methods. J Mater Sci Lett 2001:2095–6.
[34] D3822, D3822M, ASTM. Standard test method for tensile properties of polymer matrix composite materials.“ ASTM International. 28. ASTM D3822/D3822M (2014). ”Standard test method for tensile properties of polymer matrix composite materials. West Conshohocken, USA: ASTM International; 2014.
[35] D3039, D3039M. Standard Test Method for Tensile Properties of Polymer Matrix Composite Material standards. ASTM Standard; 2008.
[36] Saura-Calixto, F.,Că nellas, J.,&Garcia-Raso,J. Determination of hemicellulose, cellulose and lignin contents of dietary fibre and crude fibre of several seed hulls. Data comparison. Zeitschrift fürLebensmittel-Untersuchungund –Forschung 200–202; 1983.
[37] Yusriah L, Sapuan SM, Zainudin ES, Mariatti M. Characterization of physical, mechanical, thermal, and morphological properties of agro-waste betel nut (Areca catechu) husk fiber. J Cleaner Prod 2014:174–80.
[38] Razali N, Salit MS, Jawaid M, Ishak MR, Lazim Y. A study on chemical composition, physical, tensile, morphological, and thermal properties of roselle fiber: Effect of fiber maturity. BioResources 2015:1803–23.
[39] ISO62:2008. n.d. “Plastics - Determination of water absorption.” ISO Standards.
[40] Sen Burak, Kucukvar Murat, Onat Nuri C, Tatari Omer. Life cycle sustainability assessment of autonomous heavy-duty trucks. J Ind Ecol 2020;24(1):149–64.
[41] Onat Nuri, Kucukvar Murat, Halog Anthony, Cloutier Scott. “Systems Thinking for Life Cycle Sustainability Assessment: A Review of Recent Developments, Applications, and Future Perspectives. Sustainability 2017;9(5):706. https://doi.org/10.3390/su9050706.
[42] Kucukvar Murat, Gumus Serkan, Egilmez Gokhan, Tatari Omer. Ranking the sustainability performance of pavements: An intuitionistic fuzzy decision-making method. Autom Constr 2014;40:33–43.